This is an *Accepted Manuscript*, which has been through the Royal Society of Chemistry peer review process and has been accepted for publication.

Accepted Manuscripts are published online shortly after acceptance, before technical editing, formatting and proof reading. Using this free service, authors can make their results available to the community, in citable form, before we publish the edited article. We will replace this *Accepted Manuscript* with the edited and formatted *Advance Article* as soon as it is available.

You can find more information about *Accepted Manuscripts* in the **Information for Authors**.

Journal Name

COMMUNICATION

Silkworm Cocoons by Cylinders Self-Assembled from H-Shaped Alternating Polymer Brushes

Qiutong Huang,[a] Bo Yang,[a] Huanhuan Liu,[b] Youliang Zhao[b]* and Jianzhong Du[a]*

We report a novel silkworm cocoon-like nanostructure based on the 3D hierarchical self-assembly of cylinders which are spontaneously formed by an H-shaped polymer brush comprising a disulfide-bridged spacer (*ca.* 2 nm) and two brushes (*ca.* 2 nm) with alternating poly(ethylene glycol) and poly(ε-caprolactone) side chains [(PEG$_{16}$-*alt*-PCL$_{21}$)$_4$-S-S-(PEG$_{16}$-*alt*-PCL$_{21}$)$_4$].

Hierarchical structures by self-assembly of nanoparticles can provide properties far beyond the individual particles.[1, 2] It is well known that linear polymers can self-assemble into a variety of nanoparticles such as spherical solid micelles,[3] short worms,[4, 5] long cylinders,[6-8] toroids,[9] lamellae,[10] and hollow nanoparticles,[11-17] *etc*. Comb-like polymer brushes composed of a linear backbone with densely grafted side chains can also spontaneously form various nanostructures, providing potential applications in sensing, imaging and biomedical fields, *etc*.[18-23] Usually, the self-assembly process can be controlled by solvent properties,[2, 24] chemical structures, hydrophilic/hydrophobic ratios, concentrations of polymers,[25] and crystallizations of polymers.[26-28] For example, Manners *et al.* prepared a class of crystallization-driven cylindrical diblock copolymer micelles and co-micelles.[6] O'Reilly and coworkers reported the self-assembly of poly(lactide)-containing block copolymers through a thermally controlled crystallization.[29] To the best of our knowledge, 3D complex nanostructures such as a silkworm cocoon evolved from primary building blocks (such as polymers) to intermediate 1D and 2D building blocks (such as cylinders and cylinder raft) and then final 3D morphology in one step has not been reported.

In this communication, we present the preparation and possible mechanism insight of a novel 3D silkworm cocoon-like

nanostructure (Fig. 1 and Scheme 1) spontaneously formed by 1D cylinders which are self-assembled from an H-shaped polymer brush [(PEG$_{16}$-*alt*-PCL$_{21}$)$_4$-S-S-(PEG$_{16}$-*alt*-PCL$_{21}$)$_4$, Polymer **1** in Scheme 1] in DMF/water (1:2, v/v) solvent mixture.
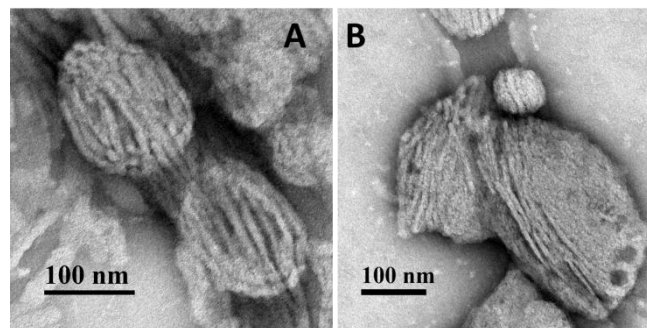
Fig. 1. TEM images of silkworm cocoons by cylinders self-assembled from disulfide-bridged H-shaped (PEG$_{16}$-*alt*-PCL$_{21}$)$_4$-S-S-(PEG$_{16}$-*alt*-PCL$_{21}$)$_4$ polymer brushes (Polymer **1**).

The H-shaped Polymer **1** comprises a disulfide-linked spacer bridging two short brushes with relatively long poly(ethylene glycol) (PEG) and poly(ε-caprolactone) (PCL) grafts. Although its structure seems complex, this polymer brush can be prepared by one-pot reversible addition-fragmentation chain transfer (RAFT) copolymerization of vinylbenzyl-terminated PEG (DP$_{PEG}$ ≈ 16) and maleimidic PCL (DP$_{PCL}$ ≈ 21) mediated by disulfide-linked RAFT agent[23] under optimized conditions (Scheme S1 in the electronic supplementary information, †ESI). The synthetic procedure is easier than our previous two-step synthetic protocol.[30] Typical gel permeation chromatography, IR spectrum and ^{1}H NMR data of this polymer brush are provided in Table S1†, Fig. S1†-Fig. S4†).

Journal Name

COMMUNICATION
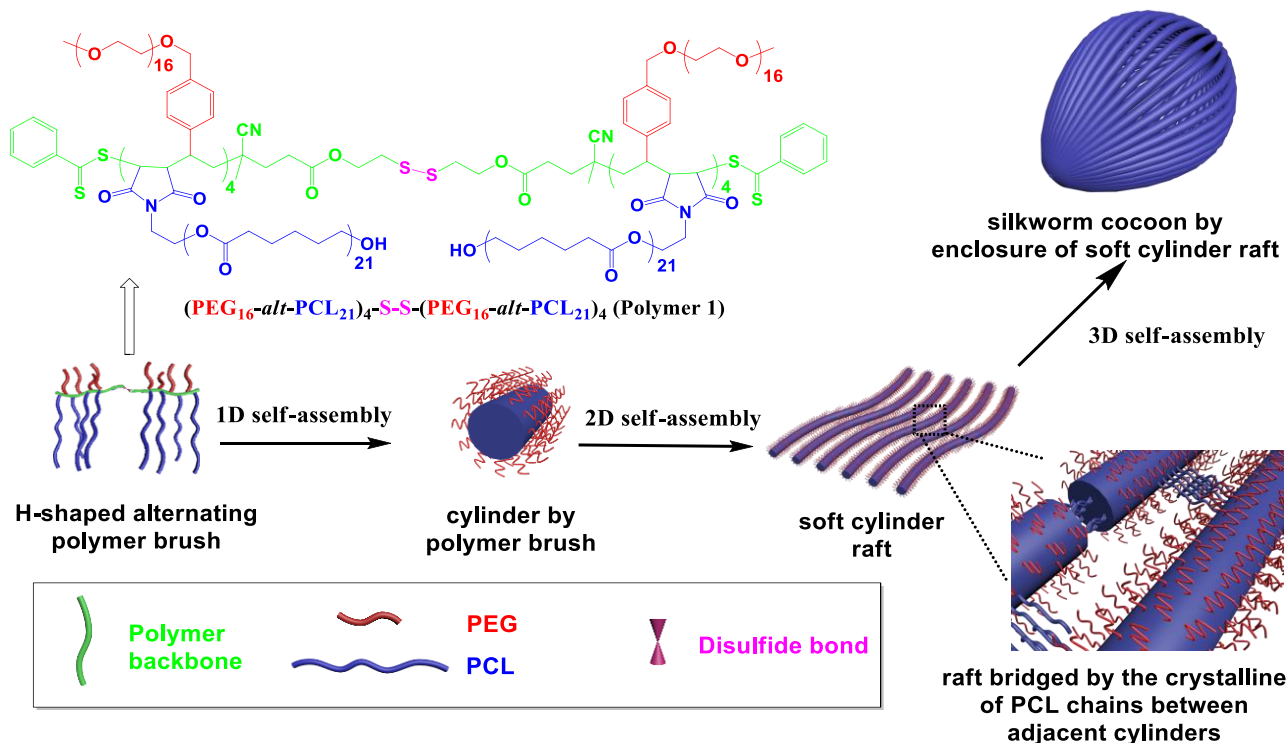
Scheme 1. Formation of a silkworm cocoon by hierarchical self-assembly of cylinders from H-shaped polymer brushes.

It is noteworthy that this disulfide-linked Polymer **1** can be easily cleaved upon DTT-triggered reduction to form a smaller (PEG$_{16}$-*alt*-PCL$_{21}$)$_4$–SH brush (Polymer **2**) without a spacer. Polymer **2** has half of the original molecular weight of Polymer **1**. The GPC curves in Fig. 2 reveals that the molecular weights of Polymer **1** (before cleavage) and Polymer **2** (after cleavage) are 30500 and 15000 with very low PDIs of 1.14 and 1.16 respectively, confirming the complete cleavage of Polymer **1**. The molecular weights of both polymers by GPC are very close to that by ^{1}H NMR (30900 and 15450, respectively). Polymer **1** has 8 hydrophilic PEG side chains (average countour length *ca.* 6 nm) and 8 partially hydrophobic PCL side chains (*ca.* 18.4 nm).[31-35] The countour length of the main chain is *ca.* 7.4 nm. The total molecular weight of 8 hydrophilic PEG chains is 6000 and the molecular weight of partially hydrophobic parts is 24900.

Compared to other techniques such as scanning electron microscopy and atomic force microscopy (data are not shown), transmission electron microscopy (TEM) is an excellent technique to present the fine nanostructure of a silkworm cocoon (Fig. 1A-B). Fig. 3A shows the occasionally trapped cylinder raft, which is perhaps the intermediate morphology during the silkworm cocoon formation. In Fig. 3B, there are three silkworm cocoons (200~400

nm) woven by cylinders. The two blue arrows indicate the local area stained by more phosphotungstic acid stains (see Fig. S5† for magnified TEM images). In Fig. 1A, there are 4 silkworm cocoons located in different focal planes. In Fig. 1B, there is a twisted silkworm cocoon and a small "satellite" silkworm cocoon. In Fig. S6†, a broken silkworm cocoon and a partially broken silkworm cocoon are clear. The red arrows in Fig. 3B indicate a slightly broken silkworm cocoon with a fringe. The mean diameter of the cylinders is approximately 16.5 nm by TEM (Fig. S6†).

Although it seems difficult to understand this spontaneous self-assembly process, we are still able to probe the possible mechanism based on the broken silkworm cocoons (Fig. S6†) and the occasionally trapped intermediate state (cylinder raft in Fig. 3A) during the evolution of a silkworm cocoon (Fig. 4) from Polymer **1**, and the control experiments with Polymer **2** (Fig. 5).

The silkworm cocoon may be formed by the following mechanism: *First,* Polymer **1** self-assembles into cylinders in DMF/water mixture (Scheme 1 and TEM image in Fig. 3A). As gradually adding water into the DMF solution, the polarity of the solvent mixture becomes higher and higher. As a result, the partially hydrophobic PCL segments (*ca.* 18.4 nm) aggregate to form the crystalline axis of the cylinder (16.5 nm of diameter), surrounding by

relatively short hydrophilic PEG coronas (*ca.* 6 nm).[34, 35] In this process, some PCL chains tend to be aligned along the axis direction and connect to each other, leading to the continuous growth of the cylinder axis (Scheme 1). In the meanwhile, other PCL chains may spread out along the direction perpendicular to the cylinder axis because the countour length of the PCL chains is *ca.* 18.4 nm, which is longer than the diameter of the cylinder core (*ca.* 16.5 nm). *Second,* during the growth of the linear cylinder along the axis direction, partial PCL chains perpendicular to the cylinder axis join the crystallization in the adjacent PCL axis, leading to the physical bridging of adjacent cylinders, which can be clearly viewed by TEM in Fig. 4. The in parallel alignment of cylinders forms a soft cylinder raft (Scheme 1 and Fig. 3A). *Finally,* a 3D silkworm cocoon is formed upon the closure of the soft cylinder raft (Fig. 1A-B and Fig. 4).

Alternatively, the PEG chains may just be too short and too loosely grafted to prevent aggregation of cylinders in side-by-side fashion by solvophobic interactions. This could further facilitate the raft formation due to optimization of packing of hydrophilic chains (sticking out to the top and bottom), while solvophobic interface is minimized due to side-by-side packing (which is consistent with the classical energy minimization in self-assembly driven by solvophobic interactions).
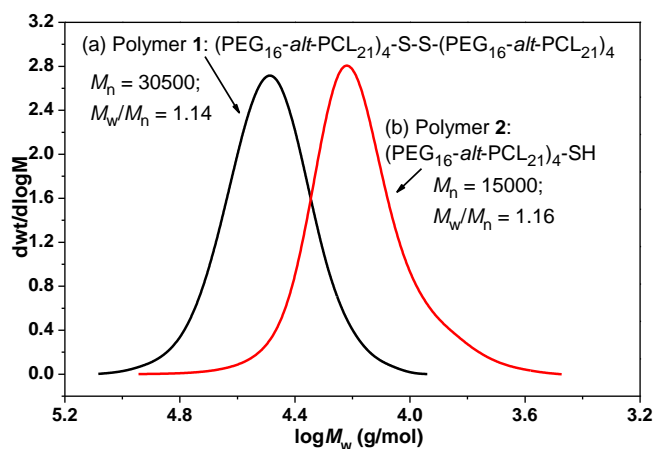

Fig. 2. GPC traces of Polymer **1** before (a) and after (b) DTT-triggered reduction. Polymer **2** is obtained after cleavage of Polymer **1**.

The silkworm cocoon is much different from the lamellar microdomain structure of conventional polymer brushes which grew from a special substrate,[36-39] or the nanostructure from hydrogen-bonded thermostable liquid crystalline complex.[40] The previous research revealed that the crystallization of PCL segments could be produced under different conditions, such as different PCL content,[41] different temperature[42] and different initial polymer concentration.[6]

In our case, we find that the disulfide-bridged H-shaped molecular structure of the polymer brush is crucial for the silkworm cocoon formation. For example, $(PEG_{16}$-*alt*-$PCL_{21})_4$–SH brush (Polymer **2**) obtained by complete cleavage of Polymer **1** doesn't have an H shape. It only forms long cylinder rafts, as confirmed by TEM studies in Fig. 5 and Fig. S7†. Dynamic light scattering (DLS)

studies in Fig. 6 revealed the D_h of cylinders rafts from Polymer **2** (282 nm) is bigger than that of silkworm cocoons from Polymer **1** (253 nm). Besides, TEM studies also confirmed that Polymer **2** affords longer cylinders than Polymer **1** (Fig. 3 and Fig. 5). Compared with cylinders from Polymer **2**, the disulfide-bridged spacer in the backbone of the H-shaped polymer **1** provides better flexibility of the cylinders due to the presence of plenty of rotational S-S bonds (there are *ca.* 3100 disulfide bonds in a 500 nm of cylinder, see the ESI for calculations),[33] which facilitates the formation of the silkworm cocoon and consequently leads to a smaller Dh. The above preliminary results indicated the important influence of the structure of polymer brushes on the final morphologies. Further self-assembly studies by varying the molecular structure of the polymer brushes are ongoing in our lab, which will be reported in the forthcoming papers.
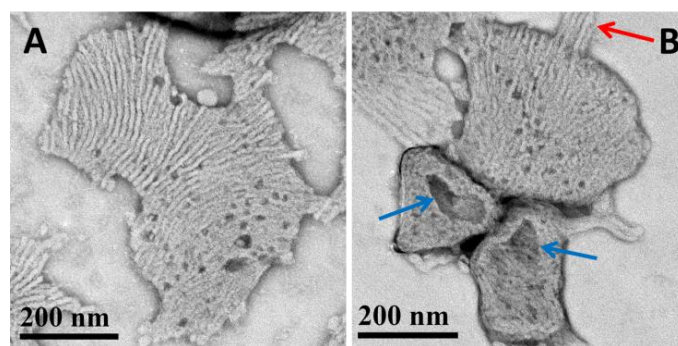

Fig. 3. TEM images of occasionally trapped cylinder raft (the intermediate state in the process of creating a silkworm cocoon) by polymer **1** in DMF/water (1:2, v/v) at an initial copolymer concentration of 1.0 mg/mL. Red arrows indicate the evidence for the enclosure of cylinder rafts. The diameter of a cylinder is *ca.* 16.5 nm.
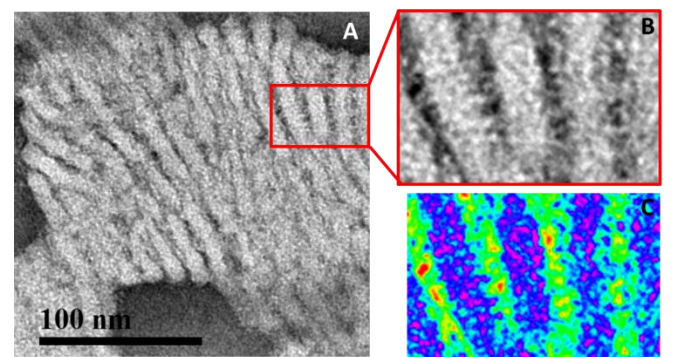

Fig. 4. (A-B) TEM image of a silkworm cocoon by cylinders, showing the physical bridges of adjacent cylinders. (C) Inverse fast Fourier transform (IFFT) image of physical bridges between cylinders.
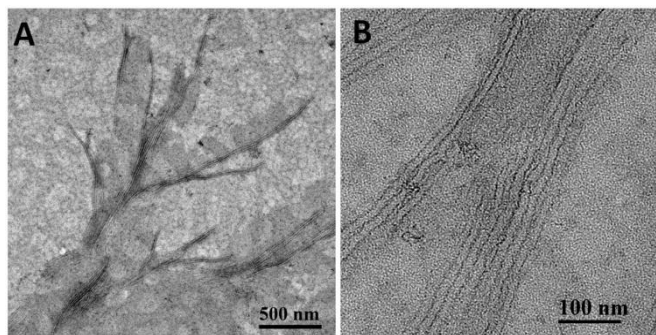
Fig. 5. TEM images of cylinder raft self-assembled by $(PEG_{16}\text{-}alt\text{-}PCL_{21})_4$–SH brush (Polymer **2**) without a disulfide-bridged spacer. The diameter of a cylinder is *ca.* 16.5 nm.

It is noteworthy that most of cylinders in Fig. 3 align together in parallel, forming cylinder rafts and then silkworm cocoons. No individual cylinders are observed, indicating the growth and the bridging processes of the cylinders from Polymer **1** occurred at the same time. This mechanism has been also verified by self-assembly of polymer **2**. Fig. 5 also revealed the cylinder raft was formed by self-propagation of polymer **2** and inter-bridging between different cylinders. In the self-propagation process, the crystalline PCL side chains (*ca.* 18.4 nm of countour length) form interdigitated cylinder axis and self-propagate along the axis to form long cylinders. The diameter of the cylinder by TEM is also *ca.* 16.5 nm, which is shorter than the countour length of the PCL side chains. Therefore, it is very likely to bridge the adjacent cylinders by the crystallization of PCL chains in the adjacent cylinder axis.
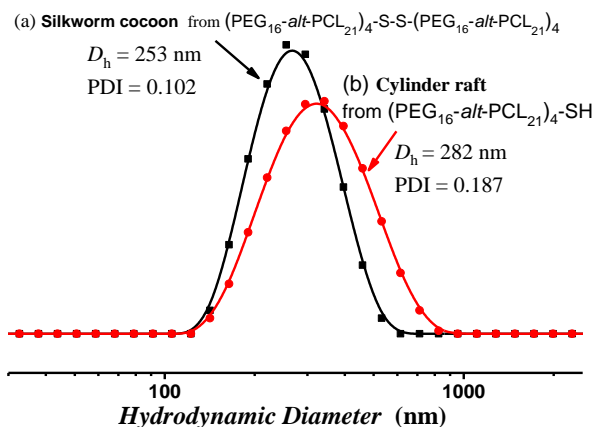

Fig. 6. Intensity-averaged size distribution determined by DLS: (a) Silkworm cocoon from Polymer **1**; (b) Cylinder raft from Polymer **2**.

In summary, we have developed a novel strategy for easily creating silkworm cocoon-like nanostructures based on the 3D hierarchical self-assembly of cylinders which are spontaneously formed by an H-shaped polymer brush. The possible mechanism is that the H-shaped polymer brushes self-propagate into 1D cylinders and in the meanwhile the cylinders inter-connect into a 2D "soft cylinder raft" bridged by the crystalline of PCL chains between adjacent cylinders. The enclosure of the soft cylinder raft leads to the formation of a 3D silkworm cocoon. It is likely that the crystalline of the PCL side chains is

the driving force during the evolution from H-shaped polymer brushes to cylinders, cylinder rafts and then silkworm cocoons. The flexible disulfide-bridged spacer in the H-shaped polymer brush facilitates the enclosure of the soft cylinder raft into a silkworm cocoon. Overall, this unique mechanism may be extended for creating a range of hierarchical nanostructures.

Notes and references

a School of Materials Science and Engineering, Key Laboratory of Advanced Civil Engineering Materials of Ministry of Education, Tongji University, 4800 Caoan Road, Shanghai, 201804, China. Email: jzdu@tongji.edu.cn

b Suzhou Key Laboratory of Macromolecular Design and Precision Synthesis, Jiangsu Key Laboratory of Advanced Functional Polymer Design and Application, College of Chemistry, Chemical Engineering and Materials Science, Soochow University, Suzhou 215123, China. Email: ylzhao@suda.edu.cn

†Electronic Supplementary Information (ESI) available: Materials, calculations, synthesis and characterization of polymer brushes and silkworm cocoons. See DOI: 10.1039/c000000x/

1. J. Z. Du and R. K. O'Reilly, *Chem. Soc. Rev.*, 2011, 40, 2402-2416.
2. J. Z. Du and Y. M. Chen, *Angew. Chem., Int. Ed.*, 2004, 43, 5084-5087.
3. E. S. Read and S. P. Armes, *Chem. Commun.*, 2007, 3021-3035.
4. C. Ruthard, M. Schmidt and F. Grohn, *Macromol. Rapid Commun.*, 2011, 32, 706-711.
5. A. Blanazs, J. Madsen, G. Battaglia, A. J. Ryan and S. P. Armes, *J. Am. Chem. Soc.*, 2011, 133, 16581-16587.
6. X. Wang, G. Guerin, H. Wang, Y. Wang, I. Manners and M. A. Winnik, *Science*, 2007, 317, 644-647.
7. T. Isono, I. Otsuka, D. Suemasa, C. Rochas, T. Satoh, R. Borsali and T. Kakuchi, *Macromolecules*, 2013, 46, 8932-8940.
8. H. G. Cui, Z. Y. Chen, S. Zhong, K. L. Wooley and D. J. Pochan, *Science*, 2007, 317, 647-650.
9. D. J. Pochan, Z. Y. Chen, H. G. Cui, K. Hales, K. Qi and K. L. Wooley, *Science*, 2004, 306, 94-97.
10. S. W. Hong, W. Gu, J. Huh, B. R. Sveinbjornsson, G. Jeong, R. H. Grubbs and T. P. Russell, *ACS Nano*, 2013, 7, 9684-9692.
11. Y. Q. Zhu, F. Y. K. Wang, C. Zhang and J. Z. Du, *ACS Nano*, 2014, 8, 6644-6654.
12. Y. Q. Zhu, L. Fan, B. Yang and J. Z. Du, *ACS Nano*, 2014, 8, 5022-5031.
13. J. Z. Du, Y. Q. Tang, A. L. Lewis and S. P. Armes, *J. Am. Chem. Soc.*, 2005, 127, 17982-17983.
14. J. Z. Du and S. P. Armes, *J. Am. Chem. Soc.*, 2005, 127, 12800-12801.

15. J. Z. Du, Y. M. Chen, Y. H. Zhang, C. C. Han, K. Fischer and M. Schmidt, *J. Am. Chem. Soc.*, 2003, 125, 14710-14711.

16. G. H. Liu, X. R. Wang, J. M. Hu, G. Y. Zhang and S. Y. Liu, *J. Am. Chem. Soc.*, 2014, 136, 7492-7497.

17. J. Huang, C. Bonduelle, J. Thevenot, S. Lecommandoux and A. Heise, *J. Am. Chem. Soc.*, 2012, 134, 119-122.

18. Y. Shi, W. Zhu, D. D. Yao, M. L. Long, B. Peng, K. Zhang and Y. M. Chen, *ACS Macro Lett.*, 2013, 3, 70-73.

19. K. Yao, Y. Chen, J. Zhang, C. Bunyard and C. Tang, *Macromol. Rapid Commun.*, 2013, 34, 645-651.

20. X. Wu, X. X. Cai, A. Hao and J. B. Wang, *J. Chem. Eng. Data*, 2013, 58, 927-931.

21. Y. Y. Mai, L. Xiao and A. Eisenberg, *Macromolecules*, 2013, 46, 3183-3189.

22. W. Y. Gu, J. Huh, S. W. Hong, B. R. Sveinbjornsson, C. Park, R. H. Grubbs and T. P. Russell, *ACS Nano*, 2013, 7, 2551-2558.

23. M. Schappacher and A. Deffieux, *Science*, 2008, 319, 1512-1515.

24. J. Z. Du and Y. M. Chen, *Macromolecules*, 2004, 37, 5710-5716.

25. J. Z. Du and R. K. O'Reilly, *Soft Matter*, 2009, 5, 3544-3561.

26. G. Rizis, T. G. M. van de Ven and A. Eisenberg, *Angew. Chem., Int. Ed.*, 2014, 126, 9146-9149.

27. N. Xia, G. Zhang, T. Li, W. Wang, H. Zhu, Y. Chen and G. Deng, *Polymer*, 2011, 52, 4581-4589.

28. Z. M. Hudson, C. E. Boott, M. E. Robinson, P. A. Rupar, M. A. Winnik and I. Manners, *Nat Chem*, 2014, 6, 893-898.

29. N. Petzetakis, A. P. Dove and R. K. O'Reilly, *Chem. Sci.*, 2011, 2, 955-960.

30. S. X. Li, C. N. Ye, G. D. Zhao, M. J. Zhang and Y. L. Zhao, *J. Polym. Sci. Part A: Polym. Chem.*, 2012, 50, 3135-3148.

31. K. D. Zou, Q. M. Liu, J. Chen and J. Z. Du, *Polym. Chem.*, 2014, 5, 405-411.

32. Q. M. Liu, J. Chen and J. Z. Du, *Biomacromolecules*, 2014, 15, 3072-3082.

33. J. Z. Du and S. P. Armes, *Soft Matter*, 2010, 6, 4851-4857.

34. J. Z. Du and S. P. Armes, *Langmuir*, 2009, 25, 9564-9570.

35. J. Z. Du and S. P. Armes, *Langmuir*, 2008, 24, 13710-13716.

36. S. H. Cho, F. Yang, G. R. Sun, M. J. Eller, C. Clark, E. A. Schweikert, J. W. Thackeray, P. Trefonas and K. L. Wooley, *Macromol. Rapid Commun.*, 2014, 35, 437-441.

37. D. P. Sweat, M. Kim, X. Yu, S. K. Schmitt, E. Han, J. W. Choi and P. Gopalan, *Langmuir*, 2013, 29, 12858-12865.

38. M. Zhang and A. H. E. Müller, *J. Polym. Sci. Part A: Polym. Chem.*, 2005, 43, 3461-3481.

39. S. G. Boyes, A. M. Granville, M. Baum, B. Akgun, B. K. Mirous and W. J. Brittain, *Surf. Sci.*, 2004, 570, 1-12.

40. T. Yu, Y. Zhou, Y. Zhao, K. P. Liu, E. Q. Chen, D. J. Wang and F. S. Wang, *Macromolecules*, 2008, 41, 3175-3180.

41. J. Wang, W. Zhu, B. Peng and Y. M. Chen, *Polymer*, 2013, 54, 6760-6767.

42. Z.-X. Du, J.-T. Xu and Z.-Q. Fan, *Macromol. Rapid Commun.*, 2008, 29, 467-471.